Gate-tunable Supercurrent in Graphene-based Josephson Junction

D. Jeong[a], G.-H. Lee[a], Y.-J. Doh[b], H.-J. Lee[a,*]

[a] *Pohang University of Science and Technology, Pohang, Korea*
[b] *Korea University Sejong, Campus, Jochiwon, Korea*

그래핀 조셉슨 접합에서 초전류의 게이트 전압 의존성

정동찬[a], 이길호[a], 도용주[b], 이후종[a,*]

Abstract

Mono-atomic-layer graphene is an interesting system for studying the relativistic carrier transport arising from a linear energy-momentum dispersion relation. An easy control of the carrier density in graphene by applying an external gate field makes the system even more useful. In this study, we measured the Josephson current in a device consisting of mono-layer graphene sheet sandwiched between two closely spaced (~300 nm) aluminum superconducting electrodes. Gate dependence of the supercurrent in graphene Josephson junction follows the gate dependence of the normal-state conductance. The gate-tunable and relatively large supercurrent in a graphene Josephson junction would facilitate our understanding on the weak-link behavior in a superconducting-normal metal-superconducting (SNS) type Josephson junction.

Keywords : Graphene, Josephson junction, supercurrent, proximity effect

I. Introduction

Superconducting order parameter penetrates into a 'non-superconducting' material when it is in contact with a superconductor with a highly transparent interface. This superconducting proximity effect describes well the superconductivity induced in a non-superconducting material sandwiched between two superconductors [1]. This Josephson effect can also be observed in conducting nanostructures such as semiconducting nanowires [2-3] and carbon nanotubes [4].

Graphene, a single-atomic layer of graphite, with two dimensional honeycomb lattice structure, is well known for its relativistic quasiparticle transport properties arising from the linear dispersion relation [5-6]. Two-dimensionality and vanishing density of states at the Fermi level (or at the Dirac point) make it possible to easily manipulate the carrier density in graphene from hole-like to electron-like by applying an external gate voltage. Relativistic characteristics of

---

*Corresponding author.   Fax : +82 54 279 3099
e-mail : hjlee@postech.ac.kr

Dirac fermions combined with the superconductivity are theoretically expected to exhibit relativistic Josephson effects. One example is the specular Andreev reflection [7], characterized by the conservation of the chiral nature of quasiparticles when an electron is reflected into hole at a superconductor-graphene interface near the Dirac point. In addition, $I_C R_N$ product (I_C is the junction critical current and R_N the normal-state junction resistance) near the Dirac point is expected to be slightly smaller than $I_C R_N$ value away from the Dirac point [8]. But, the expectation is based on the ballistic transport situation of quasiparticles crossing the junction without impurity scattering. Graphene-based Josephson junction prepared on a silicon substrate is normally in a diffusive state due to long-range Coulomb scatterings from charged impurities on the substrate and the doping effect induced during the junction fabrication process [9]. Attempts to increase the mobility by the current annealing [10] and suspending [11] the graphene layer have been limited to non-superconducting electrodes up to present. However, a diffusive graphene Josephson junction can still provide a good platform to study the effect of weak link by the modulating carrier density of graphene between hole-like and electron-like regimes. The planar structure and the intrinsic large mobility of graphene are beneficial to obtaining a large Josephson current with highly transparent contacts compared with other nanostructure-based Josephson junctions.

II. Experiment

The mono-layer graphene sheet was exfoliated from a natural graphite single crystal onto a highly doped silicon substrate covered with a 300-nm thick SiO_2 insulating layer by using Scotch brand tape. The single-layeredness of the sheet was first examined by estimating the green-light contrast difference between the graphene sheet and the substrate under an optical microscope [12]. The single-layeredness was finally confirmed by observing the half-integer quantum Hall conductance [13] plateau ($2e^2/h$) in

electrical transport measurements with a high magnetic field (12T) at T = 50 mK. The superconducting electrodes (Ti/Al/Au: 7.5/70/5 nm) were placed on top of the mono-layer graphene sheet by e-beam patterning of PMMA resist and the following metal deposition in a vacuum chamber in the base pressure of $\sim 10^{-7}$ Torr. The distance between the source and the drain electrodes was 300 nm and the width of the graphene sheet was 2.3 μm (see Fig. 1). A narrower spacing of the graphene layer between two superconducting electrodes is desired for observing the supercurrent because the Josephson is established when the spacing of the graphene junction (L) is shorter than the superconducting phase coherence length ($2\xi_N$). For Superconductor - normal metal - superconductor (SNS) junction in a dirty limit, [$\xi_N = \sqrt{\hbar D / 2\pi k_B T}$, with D is the diffusion constant and T is the temperature] [14] ξ_N is about 400 nm for mono-layer graphene at 100 mK. Up to present, the supercurrent was observed only in a device where the junction spacing of a superconductor-graphene-superconductor (SGS) Josephson junction [15-16] is shorter than 1 μm.
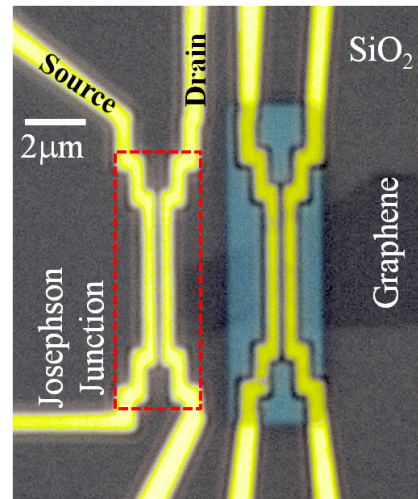

Fig. 1. The optical microscope image of the measured Josephson junction (denoted by the red dotted line). The spacing between two superconducting electrodes (Ti/Al/Au: 7.5/70/5 nm) is 300 nm and the width of exfoliated mono-layer graphene is 2.3 μm.

Data were taken by using an Oxford Instruments Model AST dilution fridge which provided a base temperature of T = 50 mK. For low-noise measurements, all measurement lines were connected to a two-stage RC-filter with the cutoff frequency ~ 30 kHz and a π-filter connected in series. The electrical conductance of the GJJ was obtained by the standard ac lock-in amplifier technique (f = 13.33 Hz) with the current bias of I_{ac} = 10 nA. The current-voltage (I-V) characteristics were obtained by sweeping the dc voltage source which was connected in series to a 30 kΩ standard resistance for the current biasing. A quasi four-probe measurement scheme was adopted for all measurements. As can be seen in Fig. 1, current was put from the source to the drain and the voltage applied to the junction was measured by using electrodes in the opposite side.
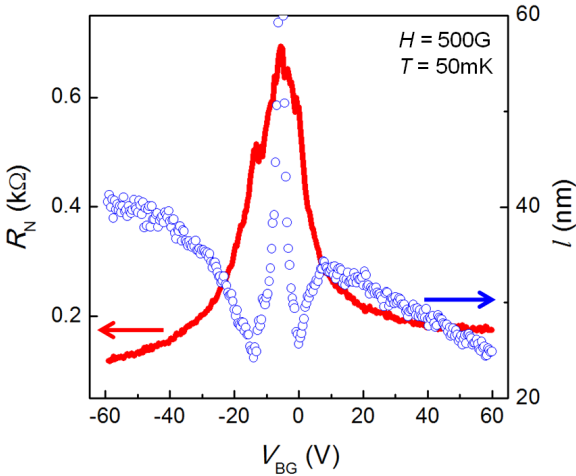

Fig. 2. Normal-state junction resistance (R_N) at H = 500 G and T = 50 mK (red line). Mean free path (l) is estimated from R_N adopting the Drude model calculation (blue circles).

Fig. 2 indicates the resistance of the graphene junction in the normal state (R_N) as a function of the back-gate voltage (V_{BG}). The normal state is achieved by quenching the superconductivity of Al electrode in an external magnetic field of H = 500 G perpendicular to the substrate (H_C ~300 G). Although both graphene junction resistance and the contact

resistance were included in the quasi four-probe measurements, resistance from the graphene is dominant over the contact resistance ~10 Ω. The R_N vs V_{BG} curve in Fig. 2 reveals a gradual transition from a hole to an electron doping states and the charge neutral point (CNP) at V_{CNP} = -5.2 V. The non-zero V_{CNP} indicates that the graphene sheet was slightly electron doped by impurities from residues during the fabrication process. We extract the charge carrier mobility (μ) and the mean free path (l) by adopting the classical Drude model calculation considering two-dimensional density of states and a linear band structure of graphene. However, the calculation collapses near the V_{CNP} by unexpected doping which is not taken into account in the Drude model. The estimated mobility (μ) is 1,800 cm^2/V·sec and corresponding mean free path (l) is 40 nm at V_{BG} = -60 V which is longer than l (V_{BG} = +60 V) = 25 nm in the electron-doped regime. The mean free path shorter than the junction spacing for all backgate voltages indicates that the quasiparticle transport in our GJJ was diffusive. Thus, the appearance of the relativistic transport of quasiparticles combined with the superconductivity, theoretically expected in graphene Josephson junction, is not adequate in this diffusive junction.

Proximity-induced superconductivity diffuses into the graphene layer between two electrodes when the junction is cooled down below the superconducting transition temperature (T_C ~ 1.2 K) of aluminum. I-V curves in Fig. 3 indicate the superconductivity which was induced by the Al superconducting electrodes. At a voltage bias higher than the Al superconducting gap energy (V > $2\Delta_{Al}$ = 250 μeV), the slope of the I-V curve in Fig. 3 is identical to the resistance obtained in Fig. 2 because Cooper pairs in the superconducting electrodes do not contribute to the voltage output. At the voltage bias below (V < $2\Delta_{Al}$), Cooper pairs from one electrode can cross the graphene junction phase-coherently and reach the other electrode by multiple Andreev reflection [17] (MAR) process. The MAR is responsible for the subgap resistance structure of V_{BG} = -14 V and -5.2 V at $V = 2\Delta/ne$ (n = ±1, ±2) in the upper left inset of Fig. 3, where Δ ~ 125 μeV is

superconducting gap of aluminum electrodes. Near zero voltage bias, graphene becomes superconducting due to the contact with electrodes. The *I-V* curve also indicates that a transition from the superconducting to the resistive state occurred when a current was increased up to the critical current (I_C). But the reverse transition occurs at the retrapping current (I_R), which gives rise to a hysteresis in the *I-V* curve.
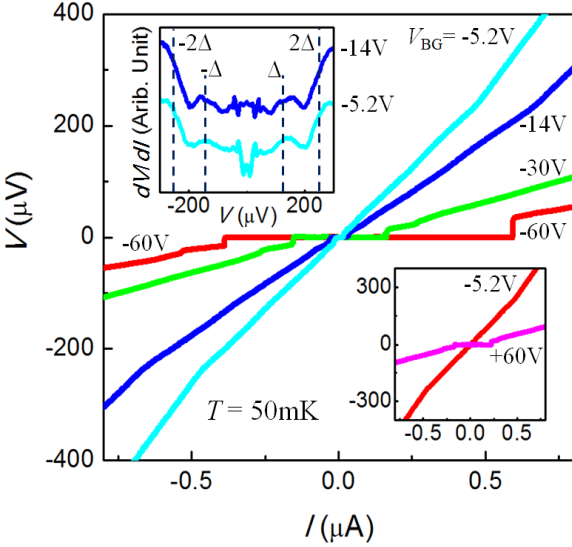

Fig. 3. *I-V* characteristics of graphene Josephson junction at various backgate voltages (V_{BG} = -60 V, -30 V, -14 V, -5.2 V from bottom to top, T = 50 mK). Lower right inset: *I-V* curves at V_{BG} = -5.2 V and 60 V, Upper left inset: dV/dI vs *V* curve at V_{BG} = -14 V and -5.2 V. The dotted lines indicate subgap structure of multiple Andreev reflection at $V = 2\Delta/ne$ ($n = \pm1, \pm2$).

Fig. 4 indicates the modulation of I_C, I_R, and G_N as the backgate voltage changes the carrier density (n) of mono-layer graphene ($n = \alpha V_{BG}$) where the capacitive coupling strength ($\alpha = 7.2*10^{10}$ cm^{-2}) is well-known in a graphene-based device with a 300-nm thick SiO$_2$ insulating layer covering the highly doped Si substrate [5].

The largest I_C is 574 nA for V_{BG} = -60 V with the largest I_R = 384 nA. I_C is gradually reduced to 155 nA and 34 nA for V_{BG} = -30 V and -14 V as the hole carrier density is decreased. The smallest I_C 18 nA at V_{CNP} = -5.2 V, increasng to 223 nA at V_{BG} = 60 V as

graphene is doped with electron carriers. The supercurrent in the hole carrier regime is larger than in the electron carrier regime with similar asymmetry in the G_N(V_{BG}) curve. The similar gate-dependence of I_C and G_N already has been reported in Josephson junctions using grapheme [15] or other nanostructures [2] as weak links. Despite of the asymmetry of I_C(V_{BG}) and G_N(V_{BG}) curve, I_C at two different V_{BG} is the same for an identical G_N. Therefore, I_C can be investigated as a function of G_N in the inset of Figs 4. However, the curve is parabolic unlike the previous report of a linear dependence [15] between I_C and G_N.
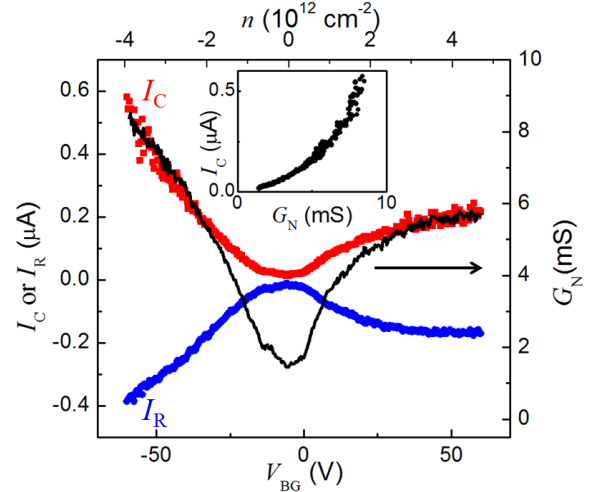

Fig. 4. Gate voltage (V_{BG}) dependence of the critical current (I_C), retrapping current (I_R) and normal state conductance (G_N) at T = 50 mK. Inset: I_C as a function G_N.

In summary, we have fabricated a Josephson junction by using mono-layer graphene and a Josephson current is observed at 50 mK, which is significantly below the Al superconducting transition temperature (1.2 K). The thinness of graphene makes easy the modulation of carrier density (n) by backgate voltage. Gate-tunable superconducting critical current (I_C) is closely related to the normal-state conductance (G_N). Gate-tunable and relative large supercurrent of graphene Josephson junction would provide a convenient system for investigating the role of weak links on the variation of the Josephson coupling strength.

Acknowledgments

References

[1] B. D. Josephson, Physics Letters **1** (7), 251-253 (1962).

[2] Y.-J. Doh, J. A. van Dam, A. L. Roest, E. P. A. M. Bakkers, L. P. Kouwenhoven and S. De Franceschi, Science **309** (5732), 272-275 (2005).

[3] J. Xiang, VidanA, TinkhamM, R. M. Westervelt and C. M. Lieber, Nat Nano **1** (3), 208-213 (2006).

[4] P. Jarillo-Herrero, J. A. van Dam and L. P. Kouwenhoven, Nature **439** (7079), 953-956 (2006).

[5] K. S. Novoselov, A. K. Geim, S. V. Morozov, D. Jiang, M. I. Katsnelson, I. V. Grigorieva, S. V. Dubonos and A. A. Firsov, Nature **438** (7065), 197-200 (2005).

[6] Y. Zhang, Y.-W. Tan, H. L. Stormer and P. Kim, Nature **438** (7065), 201-204 (2005).

[7] C. W. J. Beenakker, Physical Review Letters **97** (6), 067007 (2006).

[8] M. Titov and C. W. J. Beenakker, Physical Review B **74** (4), 041401 (2006).

[9] J. H. Chen, C. Jang, M. Ishigami, S. Xiao, W. G. Cullen, E. D. Williams and M. S. Fuhrer, Solid State Communications **149** (27-28), 1080-1086 (2009).

[10] J. Moser, A. Barreiro and A. Bachtold, Applied Physics Letters **91** (16), 163513-163513 (2007).

[11] K. I. Bolotin, K. J. Sikes, Z. Jiang, M. Klima, G. Fudenberg, J. Hone, P. Kim and H. L. Stormer, Solid State Communications **146** (9-10), 351-355 (2008).

[12] M. F. Craciun, RussoS, YamamotoM, J. B. Oostinga, A. F. Morpurgo and TaruchaS, Nat Nano **4** (6), 383-388 (2009).

[13] J. R. Williams, D. A. Abanin, L. DiCarlo, L. S. Levitov and C. M. Marcus, Physical Review B **80** (4), 045408 (2009).

[14] M. Tinkham, *Introduction to superconductivity.* (Dover Pubns, 2004).

[15] H. B. Heersche, P. Jarillo-Herrero, J. B. Oostinga, L. M. K. Vandersypen and A. F. Morpurgo, Nature **446** (7131), 56-59 (2007).

[16] X. Du, I. Skachko and E. Y. Andrei, Physical Review B **77** (18), 184507 (2008).

[17] A. F. Andreev, Sov. Phys. JETP **19**, 1228 (1964).